# A Study of the Effects of Vertical Resolution and Measurement Errors on an Iteratively Inverted Temperature Profile

MING-DAH CHOW
*Goddard Institute for Space Studies, NASA, New York, N. Y. 10025*

(Manuscript received 21 January 1974, in revised form 29 July 1974)

ABSTRACT

A direct inversion method for inverting the temperature profile from satellite-measured radiation is discussed. The $n$th power of the weighting function in the integral radiative transfer equation is used as the weight in the averaging process. The vertical resolution of the inverted temperature profile and the response of the inverted temperature profile to the measurement errors are examined in terms of $n$. It is found that for smaller values of $n$ the vertical resolution and the effect of measurement errors are reduced. When $n=0$, both the vertical resolution and error effect are minimum. The temperature profile is adjusted by a constant; any structure different from the initial shape cannot be resolved. This is equivalent to the case that the entire atmosphere is treated as one layer with a fixed shape of temperature profile. When $n \rightarrow \infty$, both the vertical resolution and error effect are maximum. This is equivalent to the case that the entire atmosphere is divided into $m$ (the number of spectral channels) layers. Within each layer, the temperatures are adjusted by a constant, and any structure different from the initial shape cannot be resolved. Also, the shape of the final solution is closer to the initial profile if the value of $n$ is smaller.

## 1. Introduction

Sensors aboard meteorological satellites measure the outgoing radiation from the earth in a number of spectral intervals. The atmospheric temperature profiles can be retrieved from the information contained in the measured radiation. Several important types of inversion techniques have been developed in the past several years. Among them are the statistical inversion technique (e.g., Strand and Westwater, 1968; Rodgers, 1970) and the direct inversion technique (e.g., Chahine, 1970; Smith, 1970). For statistical inversion techniques, the climatological mean and covariance matrix of atmospheric Planck radiance profiles for the area concerned must be known in order to obtain an optimum solution in the sense of minimum rms. For direct inversion techniques, only an initially guessed temperature profile having the same general shape as the real one is required.

In inverting a temperature profile, we would like to use a method that will resolve the true temperature structure as fine as possible. But this cannot be done due to the following two factors. One is that the maximum vertical resolution of the inverted temperature profile obtainable is restricted by the nature of the weighting functions in the integral radiative transfer equations. Usually, the shapes of the weighting function are broad, and the finestructure of the true temperature profile might not be resolvable. The other is that there is no unique solution for the temperature profile for a finite number of radiation measurements. Hence, a solution with high vertical resolution which reveals finestructures might not be useful because the finestructure would probably have little to do with the actual temperature profile. To obtain a solution comparable with the observed, an optimum solution having the general shape of the real profile is chosen. In order to do so, the temperatures at different nearby pressure levels are correlated with each other, and accordingly the vertical resolution of the inverted temperature profile is reduced.

Different sources of error are always present in the measured radiation. Since these errors might have large effects on the inverted temperature profile, it is important to reduce the effect of measurement errors. In order to reduce the effects of these errors on the inverted temperature profile, an averaging process has been used by Smith (1970). Recently, Conrath (1972) has investigated the relationship between the vertical resolution of the inverted temperature profiles and the effect of measurement errors by applying the theory of Backus and Gilbert (1970).

The vertical resolution and the effects of measurement errors depend on the particular inversion method used. Ideally, we would like to use an inversion method that increases the vertical resolution of the inverted temperature profiles and decreases the effects of measurement errors. But usually this is not possible. In Conrath's analysis, the problem of trade-off between the vertical resolution and the effect of measurement errors is investigated by assuming that the estimate of temperature is a linear combination of the measured radiances. In this study, the problem of trade-off is analyzed for a direct inversion method in which the temperature is not estimated as a linear combination of the measured radiances.

It is known that the averaging process used by Smith (1970) can reduce both the vertical resolution and the effect of measurement errors. The weights used in the averaging process are the weighting functions in the integral radiative transfer equation. In principle, the weights could be some other functions of the weighting functions in the integral radiative transfer equation. In this study, the $n$th power of the weighting function is used as the weight. The problem of trade-off between the vertical resolution and the effect of measurement errors is investigated as a function of $n$. The dependency of the final solution on the initial profile is also examined in terms of the value of $n$.

## 2. Formulations

For an atmosphere in local thermodynamic equilibrium, the outgoing radiances in $m$ spectral intervals in the longwave range can be expressed as

$$I_i=B_i(s)\tau_i(s)+\int_{\tau_i(s)}^{1} B_i[T(p)]d\tau_i(p),\quad i=1,2,\ldots,m, \tag{1}$$

where $I_i$ is the outgoing radiance in the spectral interval $i$, $B_i$ the Planck radiance, $\tau_i(p)$ the atmospheric transmission between the top of the atmosphere and the pressure level $p$, and $s$ denotes the surface. In (1), the surface is assumed to be black.

The Planck radiance in (1) is a function of wavenumber and temperature. In order to simplify the analysis of the problem of trade-off between the vertical resolution and the effect of measurement errors, the Planck radiance is linearized as a function of the Planck radiance at a fixed reference frequency $r$. As pointed out by Wark and Fleming (1966), the Planck radiance in the 15 $\mu$m $CO_2$ band can be approximated by

$$B_i(T)=\alpha_i B_r(T)+\beta_i, \tag{2}$$

where $\alpha_i$ and $\beta_i$ are linearization constants. Then (1) becomes

$$E_i=\int_{\tau_i(s)}^{1} B_r[T(p)]d\tau_i(p),\quad i=1,2,\ldots,m, \tag{3}$$

where

$$E_i=\frac{I_i-B_i(s)\tau_i(s)-\beta_i[1-\tau_i(s)]}{\alpha_i}. \tag{4}$$

For convenience, the subscript $r$ of the Planck radiance $B_r(T)$ will be omitted in the following discussions.

Assuming that the surface temperature has been determined from other sources, the inversion problem is reduced to solving the set of equations (3) for $B[T(p)]$, given the atmospheric transmission $\tau_i(p)$ and the values of $E_i$. As has been discussed by Phillips (1962) and Twomey (1965), the set of integral equations (3) is ill-conditioned. This means that if small errors are introduced in $E_i$, the solution may become unrealistic. Even if there are no errors in $E_i$, there is no unique solution of the set of equations (3) for a finite number of measurements. Because the number of measurements is always limited and errors are always introduced in the radiance measurements, an *a priori* knowledge of the real solution must exist in order to restrict the inverted temperature profile to have the general shape of the real solution. Statistical techniques make use of the mean and covariance of the Planck radiance profiles. For direct inversion techniques, the statistics of the temperature profiles are not necessary, but an initially guessed temperature profile which bears a resemblance to the real one is needed.

For an iterative method, the temperature profile of the $j$th iteration $T^j(p)$ must be known in order to calculate the temperature profile $T^{j+1}(p)$ for the next iteration. Let $E_i^j$ be the value of $E_i$ calculated from (3) with temperature profile $T^j(p)$, and $\tilde{E}_i$ be the value of $E_i$ calculated from (4) with $I_i$ equal to the satellite "measured" radiance $\tilde{I}_i$. Then the problem reduces to calculating $T^{j+1}(p)$ from $E_i^j$, $T^j(p)$, and $\tilde{E}_i$. The difference between $E_i^j$ and $\tilde{E}_i$ is due to the difference of the corresponding temperature profiles. If we assume that the difference between $E_i^j$ and $\tilde{E}_i$ has equal contributions from every portion of the atmosphere, then the profile $B[T^j(p)]$ can be adjusted by $m$ factors $\tilde{C}_i$, where $i=1, 2, \ldots, m$, to get $m$ Planck radiance profiles $B[T_i^{j+1}(p)]$ that will satisfy the $m$ measured outgoing radiances. Therefore, the profile $B[T^j(p)]$ is adjusted to $m$ new profiles as

$$B[T_i^{j+1}(p)]=\tilde{C}_i B[T^j(p)]. \tag{5}$$

The value of $\tilde{C}_i$ is chosen so as to satisfy

$$\tilde{E}_i=\int_{\tau_i(s)}^{1} B[T_i^{j+1}(p)]d\tau_i(p). \tag{6}$$

From (3), (5) and (6), the value of $\tilde{C}_i$ is given by

$$\tilde{C}_i=\tilde{E}_i/E_i^j, \tag{7}$$

and finally we get the following relaxation equation for adjusting the Planck radiance profile:

$$B^{j+1}(i,p)=B^j(p)\tilde{E}_i/E_i^j,\quad i=1, 2, \ldots, m, \tag{8}$$

where $B^{j+1}(i,p)$ and $B^j(p)$ are abbreviated versions of $B[T_i^{j+1}(p)]$ and $B[T^j(p)]$, respectively.

From (8), we have $m$ inverted Planck radiances at each pressure level. If the value of $\Delta\tau_i(p)$ (the difference of the atmospheric transmissions between the top and bottom of a layer centered at $p$) is large for a particular spectral channel $i$, then the contribution of that layer to the outgoing radiance $\tilde{I}_i$ is also large, and more information about the Planck radiance at $p$ is available from the spectral channel $i$. Therefore, the Planck radiance at each pressure level could be estimated by averaging these $m$ calculated Planck radiances weighted by some functions of $\Delta\tau_i(p)$. Smith (1970) and Chow (1974) used $\Delta\tau_i(p)$ as the weights for calculating the temperature profile. In this study, the estimate of the Planck radiance is given by

$$B^{j+1}(p)=\frac{\sum_{i=1}^{m} B^{j+1}(i,p)W_i^n(p)}{\sum_{i=1}^{m} W_i^n(p)}=\frac{B^j(p)\sum_{i=1}^{m} W_i^n(p)\tilde{C}_i}{\sum_{i=1}^{m} W_i^n(p)}, \tag{9}$$

where $W_i(p)=\Delta\tau_i(p)$, and $n$ is a positive number to be determined. As will be discussed in the following, the value of $n$ will influence the degree of vertical resolution and the effect of measurement errors.

Errors are always introduced in the measured radiances. Letting $\tilde{I}_i=I_i+e_i$, where $\tilde{I}_i$ is the measured radiance, $I_i$ the true outgoing radiance, and $e_i$ the measurement error, we then have

$$\tilde{C}_i=\frac{\{I_i-B_i(s)\tau_i(s)-\beta_i[1-\tau_i(s)]\}+e_i}{I_i^j-B_i(s)\tau_i(s)-\beta_i[1-\tau_i(s)]}=C_i+C_i^e, \tag{10}$$

where

$$C_i^e=\frac{e_i}{I_i^j-B_i(s)\tau_i(s)-\beta_i[1-\tau_i(s)]}.$$

From (9) we have

$$B^{j+1}(p)=\frac{B^j(p)\sum_{i=1}^{m} W_i^n(p)(C_i+C_i^e)}{\sum_{i=1}^{m} W_i^n(p)}. \tag{11}$$

For the case with no errors, (11) becomes

$$B^{j+1}(p)=B^j(p)F(p), \tag{12}$$

where

$$F(p)=\sum_{i=1}^{m} W_i^n(p)C_i/\sum_{i=1}^{m} W_i^n(p). \tag{13}$$

If $n=0$, then $F(p)=\sum_{i=1}^{m} C_i/m$, and the Planck radiances are adjusted by a constant. When the profile of the Planck radiance is shifted to one side, the shape of the solution exactly resembles that initially guessed. This is equivalent to the case that the entire atmosphere is considered as one layer with a fixed shape of $B(p)$. Any shape different from the initial profile cannot be resolved.

If $n$ is very large, the problem of vertical resolution can be explained with the aid of Fig. 1, which shows the curves of the weighting function $\partial\tau/\partial \ln p$ of three spectral channels. The curves of the weighting function of channels 1 and 2 intersect at 110 mb and those of channels 2 and 3 at 400 mb. If $n$ is very large, then $F(p)$ has the following values:

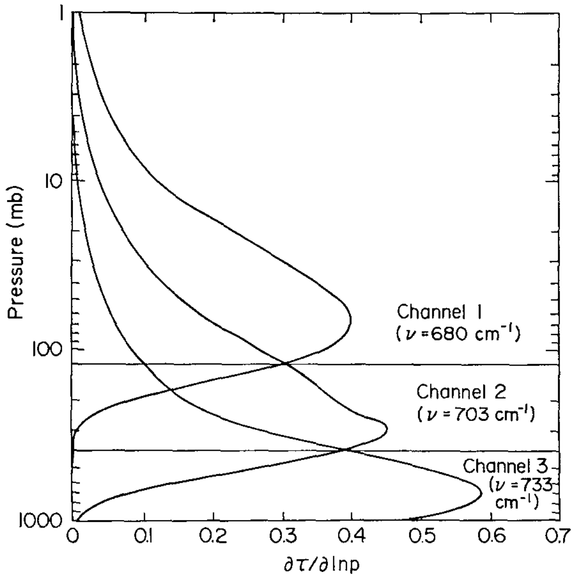


FIG. 1. Weighting functions for three channels in the 15 $\mu$m $CO_2$ band. For very large values of $n$ in (13), the atmosphere can be considered as three layers. The Planck radiances within each layer are adjusted by a constant.

$$F(p)\approx\begin{cases} C_1, & \text{for } p<110 \text{ mb} \\ C_2, & \text{for } 110 \text{ mb}<p<400 \text{ mb} \\ C_3, & \text{for } p>400 \text{ mb} \\ (C_1+C_2)/2, & \text{for } p=110 \text{ mb} \\ (C_2+C_3)/2, & \text{for } p=400 \text{ mb.} \end{cases}$$

When these three spectral channels shown in Fig. 1 are used for inverting temperature profiles, the atmosphere can be considered as three layers with interfaces located at 110 and 400 mb. The Planck radiances within each layer are adjusted by a constant: $C_1$ for the upper layer, $C_2$ for the middle layer, and $C_3$ for the lower layer. Since the Planck radiances within each layer are adjusted by a constant, the shape of the reconstructed profile within a particular layer resembles the initial profile. Therefore, within each layer any structure different from the initial shape cannot be resolved. In the neighborhood of each interface, the temperature lapse rate might be very large. However, this large temperature lapse rate can be reduced by adopting a smaller value for $n$.

Generally, if $n$ is very large and the number of spectral channels is $m$, then the atmosphere can be considered as divided into $m$ layers, and the degree of freedom for adjusting the temperature profile is $m$ (assuming that the $C$'s are independent of each other). Note that increasing the value of $m$ is equivalent to increasing the number of layers and reducing the thickness of each layer. This means that the scale of structures resolvable in the inverted temperature profile can be reduced by increasing the value of $m$. But this is not necessarily true because the $C$'s are functions of temperature profile and, accordingly, are not independent of each other.

A higher degree of freedom for adjusting the Planck radiance profile implies a higher vertical resolution of the inverted Planck radiance profile. The value of

$$\sum_{i=1}^{m} |W_i^n(p)-\overline{W_i^n(p)}|$$

measures the scatter of the coefficients in (13), where the bar denotes averaging over $i$. If this value is small, then the function $F(p)$ depends more uniformly on each $C_i$, and the values of $F(p)$ at different pressure levels are more strongly correlated. Hence, the degree of freedom for adjusting the Planck radiance profile is smaller for a smaller value of

$$\sum_{i=1}^{m} |W_i^n(p)-\overline{W_i^n(p)}|.$$

A useful measure of the degree of vertical resolution can be given as

$$v(n)=\left\{\frac{m}{2q}\sum_p \left[\sum_{i=1}^{m} |W_i^n(p)-\overline{W_i^n(p)}|/\sum_{i=1}^{m} W_i^n(p)\right]\right\}+1, \tag{14}$$

where $q$ is the number of pressure levels.

When $n=0$, then $v(n)=1$; the degree of freedom for adjusting the Planck radiance profile is 1, and the vertical resolution is minimum. When $n\rightarrow\infty$, then $v(n)=m$; the degree of freedom for adjusting the Planck radiance profile is $m$, and the vertical resolution is maximum. Note that the degree of freedom for adjusting the Planck radiance profile cannot be greater than $m$ because there are only $m$ pieces of information on the outgoing radiances.

For a smaller value of $n$, the profile $F(p)$ is closer to the constant $\sum_{i=1}^{m} C_i/m$, and from (12) the shape of the newly obtained Planck radiance profile $B^{j+1}(p)$ is closer to that of $B^j(p)$. Therefore, the solution is expected to have a character more similar to the initial profile for a smaller value of $n$.

In addition to the problem of vertical resolution, it is desirable to choose a value of $n$ that will minimize the effect of measurement errors. From (11) this value of $n$ is determined by minimizing

$$\mathrm{Var}\left[\sum_{i=1}^{m} W_i^n(p)C_i^e/\sum_{i=1}^{m} W_i^n(p)\right],$$

where Var[$x$] is the variance of $x$. With the assumption that the measurement errors $e_i$ are random and independent of each other, with means equal to zero and variances equal to $\sigma^2$, it is found that

$$\mathrm{Var}\left[\sum_{i=1}^{m} W_i^n(p)C_i^e/\sum_{i=1}^{m} W_i^n(p)\right]=\frac{\sigma^2\sum_{i=1}^{m}\left[W_i^n(p)\Big/\alpha_i\int_{\tau_i(s)}^{1} B(p)d\tau_i\right]^2}{\left[\sum_{i=1}^{m} W_i^n(p)\right]^2}.$$

Since we wish to reduce the effect of measurement errors on the inverted temperatures at all pressure levels, the problem is then reduced to minimizing the expression

$$G(n)\equiv\sum_p\left\{\frac{\sum_{i=1}^{m}\left[W_i^n(p)\Big/\alpha_i\int_{\tau_i(s)}^{1} B(p)d\tau_i\right]^2}{\left[\sum_{i=1}^{m} W_i^n(p)\right]^2}\right\}. \tag{15}$$

To simplify the analysis of the problem of trade-off between the vertical resolution and error effect, the Planck radiance has been linearized according to (2). In inverting a temperature profile, this linearization is not necessary. Instead of using (8), the relaxation equation used in the iterative scheme is

$$B_i^{j+1}(p)=B_i^j(p)\frac{\tilde{I}_i-B_i(s)\tau_i(s)}{I_i^j-B_i(s)\tau_i(s)}. \tag{16}$$

Now we have $m$ Planck radiance profiles evaluated for $m$ spectral channels, respectively. These $m$ Planck radiance profiles are transformed to another $m$ Planck radiance profiles $B^{j+1}(i,p)$ evaluated at a reference wavenumber. This procedure can be done by transforming $B_i^{j+1}(p)$ to $T^{j+1}(i,p)$ and then to $B^{j+1}(i,p)$ by using Planck's formula. Finally, the values of $B^{j+1}(p)$ are calculated from (9). For the purpose of speeding up the convergence rate, the ratio term in the right-hand side of (16) is amplified by a factor $k$, and the relaxation equation (16) is thus replaced by

$$B_i^{j+1}(p)=B_i^j(p)\left[\frac{\tilde{I}_i-B_i(s)\tau_i(s)}{I_i^j-B_i(s)\tau_i(s)}\right]^k. \tag{17}$$

The constant $k$ has a positive value. As explained by Chow (1974), suitable values of $k$ were obtained from computational trials.

## 3. Application to the 15 μm $CO_2$ band using simulated data

Seven spectral intervals centered at 668.7, 679.8, 692, 701, 709, 734 and 750 cm$^{-1}$ with a width equal to 5 cm$^{-1}$ are chosen to simulate the SIRS–B instrument on

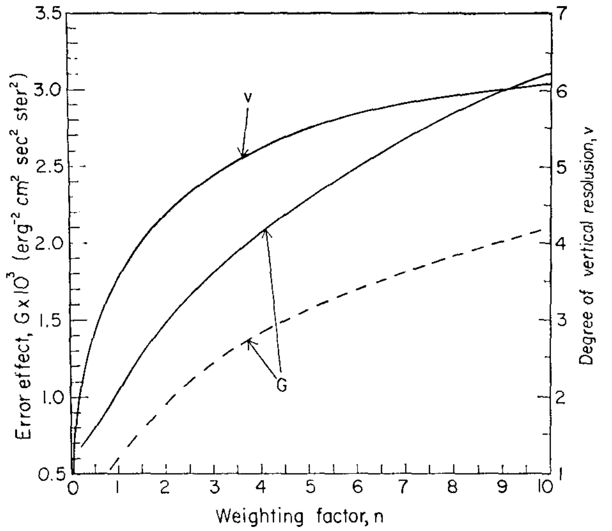


FIG. 2. Error effect and degree of vertical resolution as functions of weighting factor $n$. The solid curves are calculated by using seven spectral channels and the dashed curve is calculated from twelve spectral channels.

Nimbus 4. In this study, Drayson's (1964) calculations of the atmospheric transmission in these seven spectral intervals are used. Eighteen pressure levels shown in Fig. 3 are used for defining the temperature profile.

The degree of vertical resolution $v(n)$ calculated from (14) is shown in Fig. 2. The value of $v$ ranges from 1 for $n=0$ to the number of spectral intervals for very large $n$. It increases very rapidly at small values of $n$ and levels off as $n$ becomes large. Also shown in Fig. 2 is the error effect $G(n)$ calculated from (15) by using an ARDC model atmosphere. The value of $G$ increases with $n$. It is reduced to a minimum as $n$ is reduced to zero. Therefore, for the purpose of reducing the error effect, we would like to choose a value of $n$ as close to zero as possible, but for the purpose of increasing the degree of vertical resolution we would like to choose a value of $n$ as large as possible. This becomes a trade-off problem between the error effect and the degree of vertical resolution.

Two sample atmospheres are used for the experiment. One is in the Azores (38.75N, 27.09W) at 1200 GMT 18 May 1972. It is located at the east side of the subtropical high. This sample is designated as "Sample A." The air mass at Swan Island (17.40N, 83.93W) at the same time is a typical air mass of the tropics. The air is very hot in the surface layers and very cold at the tropopause. This is designated as "Sample B." As a first step, the outgoing radiances at the seven spectral intervals are calculated from the observed temperature profiles and the surface temperatures. These calculated outgoing radiances are then used to simulate the satellite-measured radiances $\tilde{I}_i$, either with or without introducing measurement errors.

The procedure for calculating a temperature profile given the radiance measurements and the surface temperature is to cycle through the following eight steps:

1. Guess an initial temperature profile $T^0(p)$.
2. Calculate $I_i^j$ from (1).
3. Calculate $B_i^{j+1}(p)$ from (17).
4. Calculate $T^{j+1}(i,p)$ from $B_i^{j+1}(p)$.
5. Calculate $B^{j+1}(i,p)$ from $T^{j+1}(i,p)$.
6. Calculate $B^{j+1}(p)$ from (9).
7. Calculate $T^{j+1}(p)$ from $B^{j+1}(p)$.
8. Repeat procedures 2–7 until $R_j - R_{j+1} < 0.0001$.

The residual $R_j$ of the $j$th iteration is defined as the maximum value of

$$|\{[I_i^j - B_i(s)\tau_i(s)]/[\tilde{I}_i - B_i(s)\tau_i(s)]\} - 1|, \quad i=1, 2, \ldots, m.$$

Figs. 3 and 4 show the results for Sample A with random errors introduced in the satellite "measured" radiances $\tilde{I}_i$. The random errors were generated from a Gaussian distribution function with a standard deviation of 0.5 erg cm$^{-2}$ s$^{-1}$ sr$^{-1}$ cm. The initial guess for the temperature profile is an isothermal atmosphere with a temperature equal to 273 K. Although not shown in Fig. 3, it was found that the inverted temperature profile for $n=2$, as shown in Fig. 3, is very close to the one with no errors in $\tilde{I}_i$. The effect of

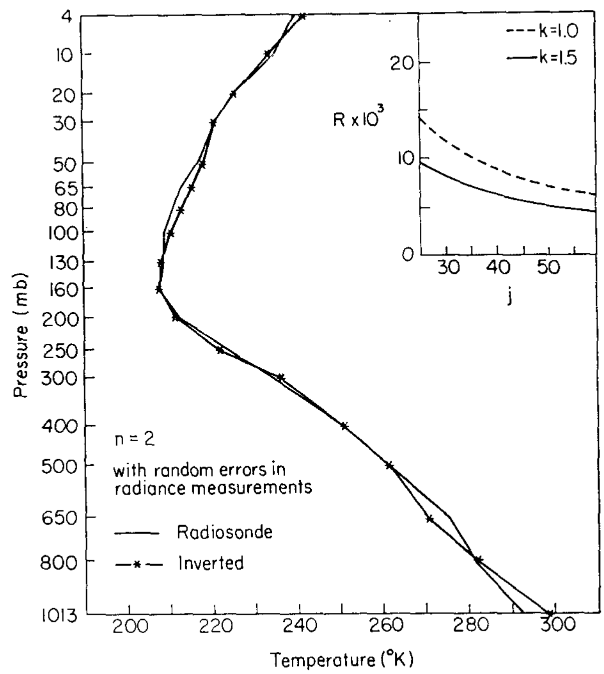


FIG. 3. Inverted temperature profile for Sample A. Random errors introduced in the "measured" outgoing radiances were generated from a Gaussian distribution function with a standard deviation of 0.5 erg cm$^{-2}$ s$^{-1}$ sr$^{-1}$ cm. $n$ is the weighting factor, $R$ the residual, $k$ the exponent that determines the convergence rate, and $j$ the number of iteration.

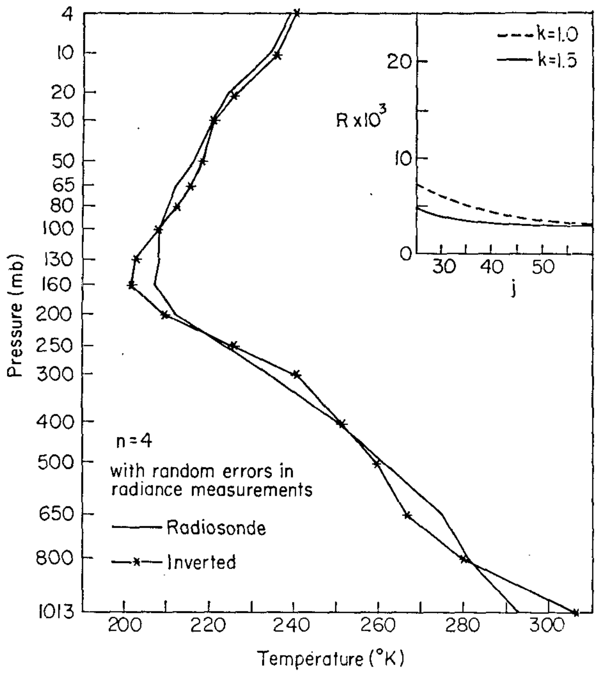


FIG. 4. As in Fig. 3 except for $n=4$.

random errors is reduced by using the weighted mean of (9). The convergence speeds of the iterative scheme are shown in the insert of Fig. 3. It can be seen from the insert that the convergence rate can be increased by changing the values of $k$. With the same values of

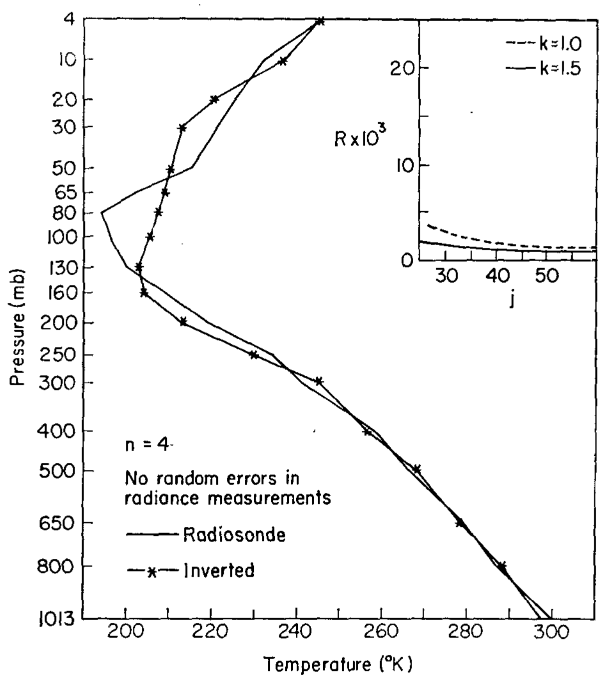


FIG. 5. Inverted temperature profile for Sample B with no errors introduced in the "measured" outgoing radiances.

$R$, the number of iterations for $k=1.5$ is only about two-thirds of that for $k=1.0$.

When the value of $n$ is increased to 4, the results are shown in Fig. 4. The deviation of the inverted temperature profile from the observed profile at the lowest layers is so pronounced that the result becomes unacceptable. The calculated air temperatures at the surface and at the 650-mb level are 15°C higher and 9°C lower, respectively, than those observed. The convergence speeds of the iterative scheme are shown in the insert of Fig. 4. Comparing the values of $R$ between Figs. 3 and 4, the convergence speeds with $n=4$ are much faster than those with $n=2$. For the case with $n=4$ and $k=1.5$, there is no essential change in $R$ after the 35th iteration.

Fig. 5 shows the results for Sample B with $n=4$. No errors are introduced in the satellite "measured" radiances. The initial guess for the temperature profile is also an isothermal atmosphere with a temperature equal to 273 K. It can be seen that the temperature profile in the neighborhood of the tropopause cannot be inverted satisfactorily, even if the value of $n$ has been increased to 4. The sharp curve of the temperature profile around the tropopause cannot be reproduced by simply increasing the value of $n$. Although increasing the value of $n$ increases the degree of vertical resolution of the inverted temperature profile, as discussed in the previous section, the resolving power is limited by the nature of the transmission functions.

Hogan and Grossman (1972) have shown that due to the nature of the transmission functions, the inverted temperature profile will bear some resemblance to the initial profile. The local sharp changes of temperature lapse rate can only be retrieved by the aid of some *a priori* knowledge. A climatological or a predicted temperature profile usually has the general features of the true one. If these profiles are used for the initial guess in the iterative scheme together with a small value of $n$, say 1, then the inverted temperature profile can be expected to bear a shape similar to that of the initial guess. For example, in the tropical area the air is hot in the surface layers and is very cold in the tropopause; in the stratosphere the temperature usually increases with height. Sample B is typical of an air mass in the tropics. Based on the above reasoning, another experiment was performed. Fig. 6 shows the results for Sample B with errors introduced in the satellite "measured" radiances. The value of $n$ is set equal to 1. A temperature profile having a similar shape as the true one is used for the initial guess. As can be seen in Fig. 6, the inverted temperature profile above the tropopause is improved, but that below the 500-mb level becomes unacceptable. The inverted temperature profile around the tropopause is similar in shape to the initially guessed profile. By examining the errors in the inverted temperature profile and in the radiance "measurements," it is found that the above-mentioned temperature error below the 500-mb level is determined by the measurement errors. Therefore, the reduction of errors from all sources ranks as one of the most significant problems in the retrieval of temperatures from satellite-measured radiances.

Although an increase in the number of spectral intervals will not necessarily provide additional information about the temperature profile, the effects of the measurement errors can be reduced. In order to examine how the number of spectral intervals will affect the solution, five additional spectral intervals centered at 675, 698, 704, 714 and 745 cm$^{-1}$, together with the original seven spectral intervals, are used to calculate the value of $G$. The values of $G$ calculated from (15) by using the seven and the twelve spectral intervals are shown in Fig. 2. It can be seen that the values of $G$ calculated from the twelve spectral intervals are smaller than those calculated from the seven spectral intervals for any value of $n$. The effect of random errors on the solution is therefore reduced.

Fig. 7 shows the inverted temperature profile for Sample B by using the twelve spectral intervals. For purposes of comparison with Fig. 6, the errors introduced in $\tilde{I}_i$ for the original seven spectral intervals are the same as those for the case shown in Fig. 6. In comparing Fig. 6 with Fig. 7, one notices that the errors in the inverted temperatures below the 500-mb level are reduced. For example, the errors in the inverted temperatures at the 500-mb level and the surface level are reduced from 6.5 to 5.0°C and from −11.0 to −6.1°C, respectively.

The number of iterations indicated in the figures would be unacceptable for practical applications. If the iteration procedure is terminated according to the magnitude of noise in the measured radiances, the number of iterations will be greatly reduced as compared to those shown in the figures.

## 4. Conclusions

The degree of vertical resolution of the inverted temperature profile and the response of the inverted temperature profile to measurement errors are discussed for a particular inversion method. These properties depend on the value of $n$ in (9). It has been shown that increasing the value of $n$ increases the degree of vertical resolution of the inverted temperature profiles, but its stability (with respect to measurement errors) is reduced. When $n=0$, the inverted temperature profiles resemble those initially guessed, and the vertical resolution is minimum. This is equivalent to the case that the entire atmosphere is considered as one layer, any structure different from the initial profile cannot be resolved.

When $n \to \infty$, both the vertical resolution and the effects of measurement errors are maximum. The atmosphere can be considered as divided into $m$ layers ($m$ is the number of spectral intervals), and the Planck radiances within each layer are adjusted by a constant. Within each layer, any structure different from the initial profile cannot be resolved.

A small value of $n$ will not only reduce the effects of

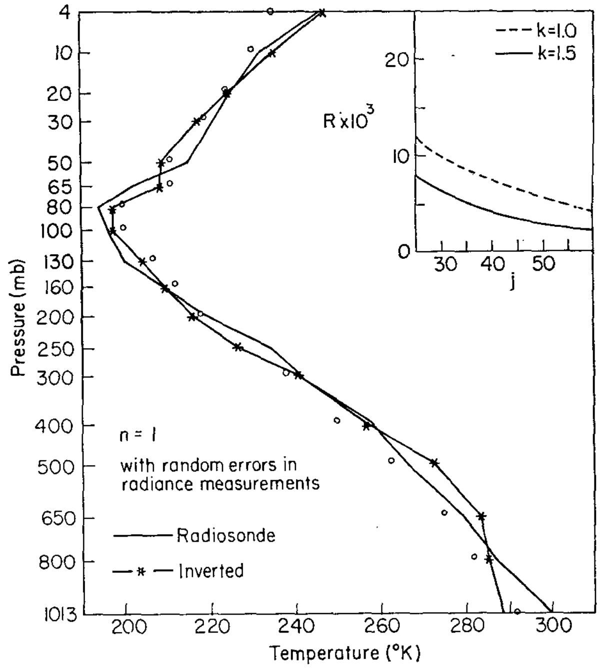


FIG. 6. Inverted temperature profile for Sample B with random errors introduced in the "measured" outgoing radiances generated from a Gaussian distribution function with a standard deviation of 0.5 erg cm$^{-2}$ s$^{-1}$ sr$^{-1}$ cm. The initially guessed temperature profile is indicated by open circles.

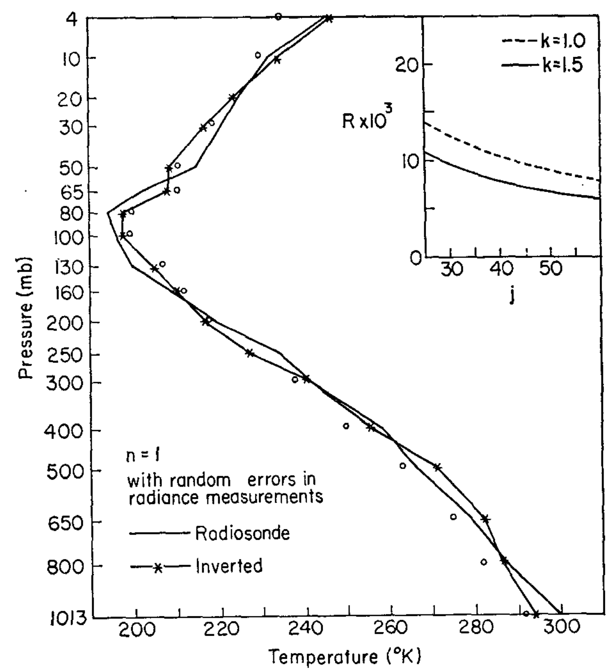


FIG. 7. As in Fig. 6 except that the number of spectral channe's used is twelve instead of seven.

measurement errors on the inverted temperature profile, but also preserve some characteristics of the initially guessed profile. If we apply the direct inversion technique to the earth's atmosphere, where a climatological or a predicted temperature profile usually has the general features of the true profile, a small value for $n$, equal to 1 or 2, is recommended. On the other hand, if we apply this technique to the atmospheres of other planets, where a good initial profile is usually not available, a larger value for $n$ should be used. This will allow the inversion scheme to have a higher degree of freedom for adjusting temperatures at different pressure levels and make the solution less dependent on the initial profile.

The computing time for inverting a temperature profile can be reduced by either adopting a suitable value of $k$ in (17) or increasing the value of $n$. Although the latter is more efficient in reducing the computing time, the quality of the inverted temperature profile might deteriorate.

*Acknowledgments.* The author wishes to thank Drs. A. Arking and J. S. Hogan and Prof. W. J. Pierson for critically reading this manuscript, and Dr. R. Jastrow for his hospitality at the Goddard Institute for Space Studies. This research was supported by a NAS-NRC Postdoctoral Research Associateship under NASA.

## REFERENCES

Backus, G., and F. Gilbert, 1970: Uniqueness in the inversion of inaccurate gross earth data. *Phil. Trans. Roy. Soc. London*, **A266**, 123–192.

Chahine, M. T., 1970: Inverse problems in radiative transfer: Determination of atmospheric parameters. *J. Atmos. Sci.*, **27**, 960–967.

Chow, M. D., 1974: An iterative scheme for determining sea surface temperatures, temperature profiles, and humidity profiles from satellite-measured infrared data. *J. Geophys. Res.*, **79**, 430–434.

Conrath, B. J., 1972: Vertical resolution of temperature profiles obtained from remote radiation measurements. *J. Atmos. Sci.*, **29**, 1262–1271.

Drayson, S. R., 1964: Atmospheric slant path transmission in the 15 $\mu$ $CO_2$ band. College of Engineering, The University of Michigan, 103 pp.

Hogan, J. S., and K. Grossman, 1972: Tests of a procedure for inserting satellite radiance measurements into a numerical circulation model. *J. Atmos. Sci.*, **29**, 797–800.

Phillips, D. L., 1962: A technique for the numerical solution of certain integral equations of the first kind. *J. Assoc. Comput. Mach.*, **9**, 84–97.

Rodgers, C. D., 1970: Remote sounding of the atmospheric temperature profile in the presence of cloud. *Quart. J. Roy. Meteor. Soc.*, **96**, 654–666.

Smith, W. L., 1970: Iterative solution of the radiative transfer equation for the temperature and absorbing gas profile of an atmosphere. *Appl. Opt.*, **9**, 1993–1999.

Strand, O. N., and E. R. Westwater, 1968: Statistical estimation of the numerical solution of a Fredholm integral equation of the first kind. *J. Assoc. Comput. Mach.*, **15**, 100–114.

Twomey, S., 1965: The application of numerical filtering to the solution of integral equations encountered in indirect sensing measurements. *J. Franklin Inst.*, **279**, 95–109.

——, 1966: Indirect measurements of atmospheric temperature profiles from satellites: II. Mathematical aspects of the inversion problem. *Mon. Wea. Rev.*, **94**, 363–366.

Wark, D. Q., and H. E. Fleming, 1966: Indirect measurements of atmospheric temperature profiles from satellites: I. Introduction. *Mon. Wea. Rev.*, **94**, 351–362.